THERMODYNAMIC PROPERTIES OF THE BINARY MIXTURE OF MONOETHANOLAMINE AND CARBON DIOXIDE

Tobias Neumann[1,2]*, Ida M. Bernhardsen[2], Hanna K. Knuutila[2], Jana P. Jakobsen[2], Roland Span[1]

[1] Lehrstuhl für Thermodynamik, Ruhr University Bochum, 44801 Bochum, Germany

[2] Department of Chemical Engineering, Norwegian University of Science and Technology, 7491 Trondheim, Norway

* Corresponding author e-mail: T.Neumann@thermo.rub.de

Abstract

Homogenous densities in the liquid phase and VLE data were measured for the monoethanolamine and carbon dioxide system. The density data were obtained on five isotherms in a temperature range between 313.15 K and 353.15 K at atmospheric pressure and for two different loadings. VLE data were acquired on the isotherms 333.15 K, 353.15 K, and 373.15 K. These new data enabled the adjustment of an e-NRTL Gibbs excess model in combination with a cubic equation of state for CO_2 to describe the gas phase. The model represents the partial pressure of CO_2 above carbon dioxide loaded pure monoethanolamine well.

Keywords: Density, phase equilibrium, measurements, monoethanolamine, carbon dioxide, e-NRTL model

1. Introduction

The global warming caused by continuously increasing concentrations of the greenhouse gas carbon dioxide in the atmosphere has to stay below a temperature increase of 1.5 °C [1] in order to prevent severe consequences of an irreversible climate change. Decreasing the CO_2 pollutions from e.g. energy or chemical industries is the main goal. Here, a key technology is carbon capture and storage (CCS). For the separation of CO_2 from for example flue gases of power plants burning fossil fuels, amine solutions are one of the most promising and mature approaches [2]. One of the most analyzed amines that is often used as a benchmark is aqueous monoethanolamine (MEA).

In most calculations and simulations, the thermodynamic properties of the multicomponent mixture $MEA + CO_2 + H_2O$ are represented with models, which are based on combinations of binary interactions of the contained components. These models are typically adjusted to ternary data. However, it is discussed if the binary parts itself are represented properly. To our knowledge there is no data available for the non-aqueous system of only $MEA + CO_2$ to check this or to enhance the adjustment of the ternary model. In order to extend the possibilities of model validation, data were experimentally measured for the binary mixture of $MEA + CO_2$. Homogeneous density data were measured for CO_2 loadings of 0.12 mol CO_2 / mol MEA and 0.22 mol CO_2 / mol MEA at atmospheric pressure on the isotherms 313.15 K, 323.15 K, 333.15 K, 343.15 K, and 353.15 K. The VLE data cover the three isotherms 333.15 K, 353.15 K, and 373.15 K. The latter ones were the basis for the development of a Gibbs excess energy model in form of the e-NRTL [3]. To describe the gas phase of the phase equilibrium data, a cubic Peng-Robinson equations of state [4] for CO_2 was used.

2. Materials and Methods

Carbon dioxide (CO_2, CAS: 124-38-9), with a purity of 99.999 % was provided by AGA and monoethanolamine (MEA, CAS: 141-43-5), with a purity of ≥99.5 %, was provided by Sigma-Aldrich. MEA was used as received. The lot numbers for MEA were STBJ2248 and STBH4366.

2.1 Density Measurements

Density measurements were performed using an Anton Paar DMA 4500 M density meter (Evjen et al. [5]). The density meter is equipped with a temperature-regulated magazine which can take up to 44 samples with 10 mL solution and an Xsample 452 for automatic filling, measuring, and cleaning. The measurements were conducted in the temperature range 313 K – 353 K and for each sample two density measurements were made, with only the average value being reported. Between every sample a control sample containing Millipore water was placed. The measurements were carried out under atmospheric pressure. However, no pressure control was used. The water measurements laid the basis for estimating the uncertainty of the density measurements.

2.2 Vapor-Liquid Equilibrium (VLE) Measurements

Vapor-liquid equilibrium (VLE) measurements were carried out using the same apparatus (Figure 1) as previously used by Hartono et al. [6]. The apparatus consists of a Büchi glass reactor and a stainless-steel gas holding vessel. The pressure in the reactor and in the vessel is measured by a pressure transmitter PTX5072, with a pressure range of 0 kPa – 600 kPa (uncertainty of ±0.15 % of the full scale), and the temperature of the gas and liquid phase is measured by Pt-100 thermometers (uncertainty of ±0.1 K).

Prior to generating VLE data for the MEA + CO₂ system, the VLE apparatus was validated by measuring the solubility of CO₂ in water. Since the experimental procedure used for validating the apparatus was slightly different from the one used to generate VLE data, the procedures are described separately.
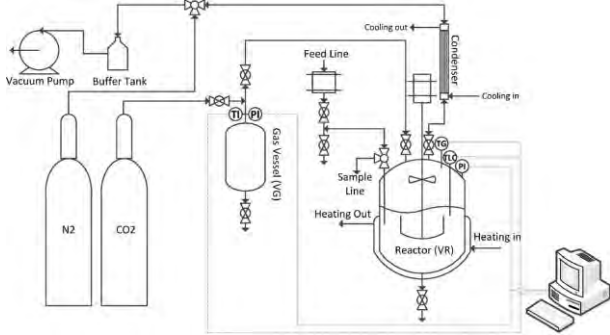

Figure 1: Illustration of the VLE apparatus. The figure is retrieved from Hartono et al. [6].

The solubility of CO₂ in water was measured in the temperature range of 313 K – 393 K and the experimental procedure was similar as described in Bernhardsen and Knuutila [7]. Briefly, the reactor was first evacuated at 293 K – 298 K, fed with a known amount of deionized water, and then evacuated again to remove potential air that entered the reactor during filling. The deionized water was then heated to desired temperatures in the range of 313 K – 393 K and, at each temperature, equilibrium was established. This resulted in a temperature-pressure profile before the addition of CO₂. At the highest experimental temperature, CO₂ was added from the gas holding vessel to the reactor. Then, the system was left to equilibrate and when equilibrium was reached, the temperature was decreased for new equilibrium points. This resulted in a temperature-pressure profile after the addition of CO₂.

At each temperature, the equilibrium partial pressure of CO₂ (p_{CO_2}) was calculated from total pressure measurements as following:

$$p_{CO_2} = p_{\text{after addition}} - p_{\text{before addition}}. \tag{1}$$

This is based on the assumption that "the partial pressure of the liquid phase remains constant and is equal to the total pressure in the reactor before the first addition of CO₂" as stated in Kim et al. [8] or in Knuutila and Nannestad [9].

The concentration of CO₂ in the liquid phase, at each temperature, was calculated as given in Eq. (2) in which the amount of CO₂ added from the gas holding vessel, $n_{CO_2}^{\text{added}}$, and present in the gas phase of the reactor, $n_{CO_2}^{\text{g}}$, was calculated using the Helmholtz energy equation of state by Span and Wagner [10].

$$c_{CO_2} = \frac{n_{CO_2}^{\text{added}} - n_{CO_2}^{\text{g}}}{V_L} \tag{2}$$

The CO₂ solubility was expressed by Henry's law constant as follows:

$$H_{CO_2} = \frac{p_{CO_2}}{c_{CO_2}}. \tag{3}$$

2.2.1 VLE Measurements of the MEA + CO₂ System

VLE data for the MEA + CO₂ system were generated in the temperature range of 333 K – 373 K and the experimental procedure was the same as described in Hartono et al. [6]. Similar as above, the reactor was first evacuated, fed with a known amount of MEA, and once again evacuated. The experiments were carried out isothermally and under stirring at the experimental temperature, the system was left to equilibrate. When a stable temperature and pressure were obtained, CO₂ was added from the gas holding vessel to the reactor. The system was once again left to equilibrate before a new portion of CO₂ was added to the reactor. This procedure was repeated until the total pressure in the reactor at the experimental temperature was around 500 kPa. At the end of the experiment, a liquid sample was collected for CO₂ and amine analysis. On average, the CO₂ loading determined from the liquid analysis deviated 2 % relative to the loading from the calculated values.

The partial pressure of CO₂ was calculated from Eq. (4) by using information about the total pressure (p_{total}) and the pressure in the reactor before the addition of CO₂ (p_{initial}).

$$p_{CO_2} = p_{\text{total}} - p_{\text{initial}} \tag{4}$$

The concentration of CO₂ in the liquid phase was, as above, calculated using Eq. (2).

3. Theory and Model Description

The phase equilibrium is described in general by the equality of the chemical potential of each component i in each of the phases:

$$\mu_i^{\text{g}} = \mu_i^{\text{l}}. \tag{5}$$

The gas phase can be described in the following manner:

$$\mu_i^{\text{g}} = RT \ln \frac{x_i^{\text{g}} \varphi_i^{\text{g}} p}{p^{\text{ref}}} + \mu_i^{\text{ref}}. \tag{6}$$

The gas constant $R = 8.314462618 \, \text{J} \cdot \text{mol}^{-1} \cdot \text{K}^{-1}$ is defined in Newell et al. [11]. The reference pressure p^{ref} is set to 1 atm. To calculate the fugacity coefficients in the gas phase φ_i^{g}, a cubic Peng-Robinson equation of state by Peng and Robinson [4] is used. Since the models for the gas and liquid phase refer to different reference states this needs to be considered in the chemical potential with μ_i^{ref}. The description of the liquid phase is accomplished with an activity coefficient approach. It reads

$$\mu_i^{\text{l}} = RT \ln \frac{x_i^{\text{l}} \gamma_i}{\gamma_i^{\infty}}. \tag{7}$$

The activity coefficients are derived from a Gibbs excess energy model in form of the e-NRTL according to Chen and Evans [3]. The model is based on the summation of short range interactions, which is a temperature dependent function of non-randomness and energy parameters and long range interactions describing electrostatic forces [3]. Similar to Monteiro et al. [12] and Putta et al. [13], the long range term is a Pitzer-Debye-Hückel term corrected by a Born term as published by Austgen et al. [14]. The parameters of the e-NTRL model

can be found in Table 1 and Table 2 in the appendix. Each of the components has an assigned reference state. For MEA the pure component reference state was chosen. Thus, γ_{MEA}^{∞} is equal to zero. CO_2 is at the reference state of a pure component in an infinite dilution of water. Because of this reference state and the general structure of the e-NRTL model, information about the contribution between water and these components are needed to calculate γ_i^{∞}. Therefore, all parameters containing water in Table 1 were adopted from a ternary e-NRTL model presented in Putta et al. [13]. It has to be noted that these parameters solely influence γ_i^{∞} because the mole fraction of water is equal to zero, which makes its influence vanish. The other parameters of the new e-NRTL model were adjusted to the VLE data reported in section 4.2 by using a particle swarm optimization algorithm from Monteiro et al. [12]. Depending on the reference state, the correction of the chemical potential in Eq. (6) for CO_2 is

$$\mu_{CO_2}^{ref} = RT \ln \frac{p^{ref}}{H_{CO_2 \text{ in } H_2O}} \qquad (8)$$

with the Henry's law constant $H_{CO_2 \text{ in } H_2O}$ taken from Carroll et al. [15] and for MEA

$$\mu_{MEA}^{ref} = RT \ln \frac{p^{ref}}{\varphi_{s,MEA} \cdot p_{s,MEA}} \qquad (9)$$

with the saturation fugacity coefficient and saturation pressure of pure MEA at the specific temperature.

The mixture of MEA + CO_2 is assumed to be reactive also without the presence of water, as stated in Han et al. [16], which can be described with the following reaction equation

$$MEACOO^- + MEAH^+ \leftrightarrow CO_2 + 2MEA. \qquad (10)$$
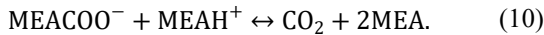
Hereby, $MEAH^+$ and $MEACOO^-$ are also at pure component reference state in an infinite dilution of water. Thus, the γ_i^{∞} used in Eq. (7) have to be calculated. The reaction is assumed to occur only in the liquid phase. Therefore, the components $MEAH^+$ and $MEACOO^-$ are not present in the gas phase and also do not require a correction of the chemical potential for the reference state in Eq. (6). The equilibrium constant K_{eq} was empirically determined during the adjustment of the e-NRTL parameters and reads:

$$K_{eq}(T) = \exp\left(A + \frac{B}{T} + C \cdot \ln(T/K) + D \cdot T \right)$$
$$\text{with } A = -137.438, B = -6661.75 \text{ K}, \qquad (11)$$
$$C = 36.5588, D = -0.19082 \text{ K}^{-1}$$

For the results shown in section 4.2, the chemical equilibrium was solved with an algorithm by Michelsen and Mollerup [17]. The algorithm minimizes the overall Gibbs energy of the system applying a Lagrange multiplier based approach. Further details can be found in Pinto [18].

4. Results

In the following section, the results of the density and VLE measurements are presented and discussed. The

VLE data are compared to the e-NRTL model with the newly adjusted parameters.

4.1 Density Data

The uncertainty and repeatability of the density measurements were 1 kg/m^3 and 10^{-2} kg/m^3, respectively. The data can be found in Table 3 in the appendix and in Figure 2 with a comparison to densities of pure MEA.
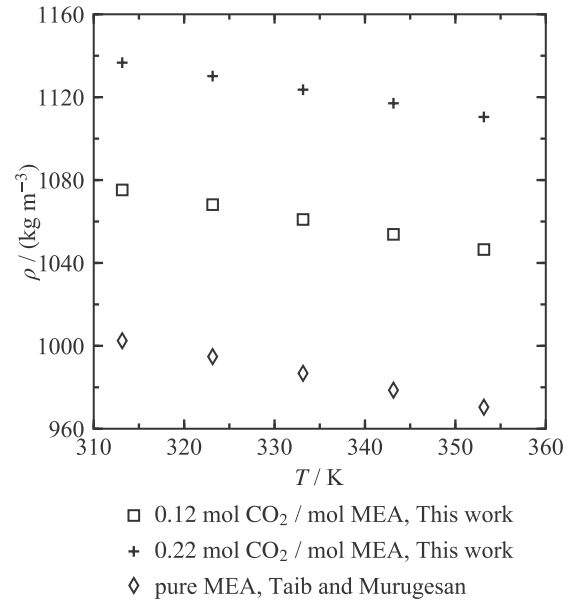
Figure 2: Homogeneous liquid densities for pure MEA [19] and CO_2 loaded 100 wt% MEA solutions at atmospheric pressure (listed in the appendix).

Similar to pure MEA, the density of the loaded solutions decreases with increasing temperature. As expected increasing the loading increases the density.

4.2 VLE Data and Model Comparison

The VLE experiments were validated by measuring the solubility of CO_2 in water in the temperature range of 40 °C – 120 °C (Figure 3, Table 4 in the appendix) and by comparing the data to the Henry's law correlation provided by Carroll et al. [15].
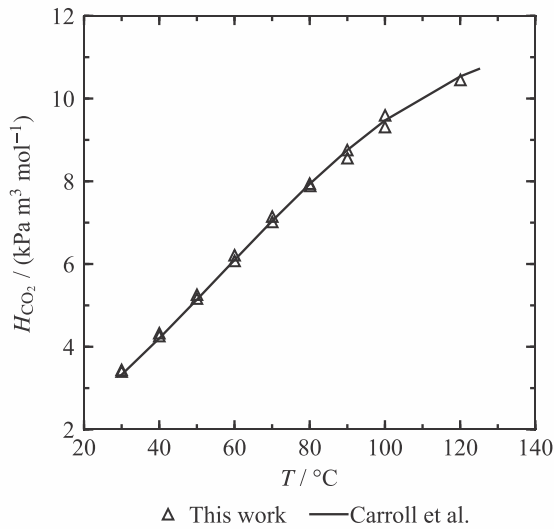
Figure 3: Experimental Henry's law constants for CO_2 in water in comparison to the correlation by Carroll et al. [15].

The average absolute relative deviation (AARD) between experimental and literature values [15] of the Henry's law constant was 1.4 % and the repeatability was on average 2 %. The VLE data are tabulated in the appendix. A comparison with the model developed in this work is shown in Figure 4.
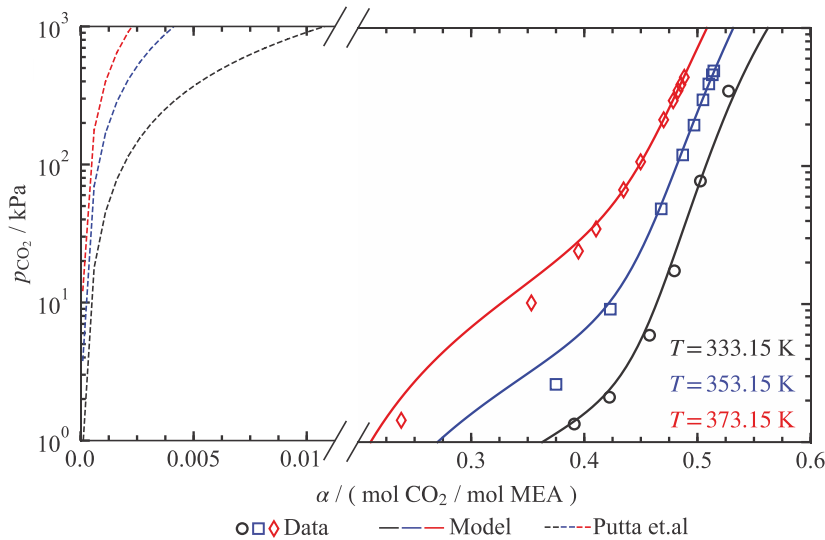

Figure 4: Experimental VLE data (listed in the appendix) in comparison to the model developed for the MEA + CO_2 system and corresponding binary parameters taken from Putta et al. [13].

The ternary model was fitted only for aqueous solutions of up to 60 wt% MEA. Since it is not possible to describe the data in Figure 4 with the corresponding binary e-NRTL parameters taken from the established e-NRTL model for the ternary system from Putta et al. [13] the adjustment of a binary model is necessary. The representation of the data with the new model is good with an AARD of 18.7 % in terms of pressure. The deviations decrease with increasing loading. Most of the data points are represented within the combined uncertainty with respect to the partial pressure of CO_2 of $u_c(p_{CO_2}) = 1.3$ kPa (cf. Table 5). Since the loading in the VLE data is greater than 0.5 mol CO_2 / mol MEA and due to the reaction equation in Eq. (10), also physical absorption has to occur. This is also captured by the new model as shown in the speciation diagram for one exemplary temperature in Figure 5.
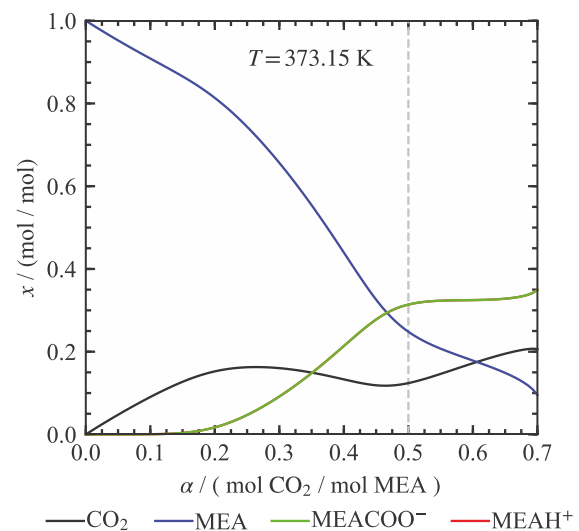

Figure 5: Speciation diagram of the developed model for the MEA + CO_2 system with respect to loading of CO_2.

The compositions of MEAH$^+$ and MEACOO$^-$ are the same because of the equality of charge. Therefore, the green and red line overlap exactly. The CO_2 is first physically absorbed until a loading of around 0.2 mol CO_2 / mol MEA when the reaction starts increasing the amount of MEAH$^+$ and MEACOO$^-$. This is also visible by the steeper decrease of MEA. At a loading of around 0.5 mol CO_2 / mol MEA, the concentrations of MEAH$^+$ and MEACOO$^-$ become almost constant and CO_2 starts to increase again.

5. Conclusion

The binary system of MEA + CO_2 was experimentally investigated and described in terms of a Gibbs excess model. Homogeneous density data points in the liquid phase were measured for two loadings at atmospheric pressure in a temperature range of 313.15 K – 353.15 K. The data were compared to densities of pure MEA. VLE measurements at atmospheric pressure ranges in loadings from 0.238 mol CO_2 / mol MEA to 0.528 mol CO_2 / mol MEA and the temperature from 333.15 K to 373.15 K. The combined standard uncertainty with regard to partial pressure of CO_2 is calculated to 1.3 kPa. An e-NRTL model for the liquid phase was adjusted to the VLE data considering the assumed reactive nature of the mixture forming protonated MEA and carbamate. The representation of the data with the model is qualitatively good. In most cases the experimental uncertainty could be matched. Since only the binary contributions from an established ternary model do not match the data an enhancement of the ternary models using the non-aqueous MEA + CO_2 data obtained in this work is an exciting idea for future work. The speciation shows a combination of chemically and physically absorbed CO_2 in the liquid, which is confirmed by the VLE data.

Acknowledgements

References

[1] IPCC, Global warming of 1.5 °C, (2019). https://www.ipcc.ch/sr15/.

[2] G.T. Rochelle, Amine Scrubbing for CO2 Capture, Science (80-.). 325 (2009) 1652–1654. https://doi.org/10.1126/science.1176731.

[3] C. -C Chen, L.B. Evans, A local composition model for the excess Gibbs energy of aqueous electrolyte systems, AIChE J. 32 (1986) 444–454. https://doi.org/10.1002/aic.690320311.

[4] D.Y. Peng, D.B. Robinson, A New Two-Constant Equation of State, Ind. Eng. Chem. Fundam. 15 (1976) 59–64. https://doi.org/10.1021/i160057a011.

[5] S. Evjen, R. Wanderley, A. Fiksdahl, H.K. Knuutila, Viscosity, Density, and Volatility of Binary Mixtures of Imidazole, 2-Methylimidazole, 2,4,5-Trimethylimidazole, and 1,2,4,5-Tetramethylimidazole with Water, J. Chem. Eng. Data. 64 (2019) 507–516. https://doi.org/10.1021/acs.jced.8b00674.

[6] A. Hartono, R. Rennemo, M. Awais, S.J. Vevelstad, O.G. Brakstad, I. Kim, H.K. Knuutila, Characterization of 2-piperidineethanol and 1-(2-hydroxyethyl)pyrrolidine as strong bicarbonate forming solvents for CO 2 capture, Int. J. Greenh. Gas Control. 63 (2017) 260–271. https://doi.org/10.1016/j.ijggc.2017.05.021.

[7] I.M. Bernhardsen, H.K. Knuutila, A review of potential amine solvents for CO2 absorption process: Absorption capacity, cyclic capacity and pKa, Int. J. Greenh. Gas Control. 61 (2017) 27–48. https://doi.org/10.1016/j.ijggc.2017.03.021.

[8] I. Kim, K.A. Hoff, T. Mejdell, Heat of absorption of CO2 with aqueous solutions of mea: New experimental data, Energy Procedia. 63 (2014) 1446–1455. https://doi.org/10.1016/j.egypro.2014.11.154.

[9] H.K. Knuutila, Å. Nannestad, Effect of the concentration of MAPA on the heat of absorption of CO2 and on the cyclic capacity in DEEA-MAPA blends, Int. J. Greenh. Gas Control. 61 (2017) 94–103. https://doi.org/10.1016/j.ijggc.2017.03.026.

[10] R. Span, W. Wagner, A New Equation of State for Carbon Dioxide Covering the Fluid Region from the Triple-Point Temperature to 1100 K at Pressures up to 800 MPa, J. Phys. Chem. Ref. Data. 25 (1996) 1509–1596. https://doi.org/10.1063/1.555991.

[11] D.B. Newell, F. Cabiati, J. Fischer, K. Fujii, S.G. Karshenboim, H.S. Margolis, E. de Mirandés, P.J. Mohr, F. Nez, K. Pachucki, T.J. Quinn, B.N. Taylor, M. Wang, B.M. Wood, Z. Zhang, The CODATA 2017 values of h , e , k , and N A for the revision of the SI, Metrologia. 55 (2018) L13–L16. https://doi.org/10.1088/1681-7575/aa950a.

[12] J.G.M.-S. Monteiro, D.D.D. Pinto, S.A.H. Zaidy, A. Hartono, H.F. Svendsen, VLE data and modelling of aqueous N,N-diethylethanolamine (DEEA) solutions, Int. J. Greenh. Gas Control. 19 (2013) 432–440. https://doi.org/10.1016/j.ijggc.2013.10.001.

[13] K.R. Putta, D.D.D. Pinto, H.F. Svendsen, H.K. Knuutila, CO2 absorption into loaded aqueous MEA solutions: Kinetics assessment using penetration theory, Int. J. Greenh. Gas Control. 53 (2016) 338–353. https://doi.org/10.1016/j.ijggc.2016.08.009.

[14] D.M. Austgen, G.T. Rochelle, X. Peng, C.C. Chen, Model of Vapor—Liquid Equilibria for Aqueous Acid Gas—Alkanolamine Systems Using the Electrolyte—NRTL Equation, Ind. Eng. Chem. Res. 28 (1989) 1060–1073. https://doi.org/10.1021/ie00091a028.

[15] J.J. Carroll, J.D. Slupsky, A.E. Mather, The Solubility of Carbon Dioxide in Water at Low Pressure, J. Phys. Chem. Ref. Data. 20 (1991) 1201–1209. https://doi.org/10.1063/1.555900.

[16] B. Han, Y. Sun, M. Fan, H. Cheng, On the CO 2 Capture in Water-Free Monoethanolamine Solution: An ab Initio Molecular Dynamics Study, J. Phys. Chem. B. 117 (2013) 5971–5977. https://doi.org/10.1021/jp4022932.

[17] M.L. Michelsen, J. Mollerup, Thermodynamic Models: Fundamentals & Computational Aspects, Tie-

Line Publications, 2007.

[18] D.D.D. Pinto, CO2 capture solvents: modeling and experimental characterization, Ph.D. Thesis, Norwegian University of Science and Technology, 2014.

[19] M.M. Taib, T. Murugesan, Density, Refractive Index, and Excess Properties of 1-Butyl-3-methylimidazolium Tetrafluoroborate with Water and Monoethanolamine, J. Chem. Eng. Data. 57 (2012) 120–126. https://doi.org/10.1021/je2007204.

[20] K.S. Pitzer, Electrolytes. From dilute solutions to fused salts, J. Am. Chem. Soc. 102 (1980) 2902–2906. https://doi.org/10.1021/ja00529a006.

Appendix

Table 1: e-NRTL parameters of the short range terms for the system MEA + CO$_2$ with water being apparent for the reference state of infinite dilution. The non-randomness parameters were fixed to 0.2.

Molecular Parameters: $a_{m,m}$ and $b_{m,m}$			
a_{H_2O,CO_2}	0 [a]	b_{H_2O,CO_2}	0 [a]
$a_{H_2O,MEA}$	-1.2024 [a]	$b_{H_2O,MEA}$	281.3086 [a]
a_{CO_2,H_2O}	0 [a]	b_{CO_2,H_2O}	0 [a]
$a_{CO_2,MEA}$	0.86900	$b_{CO_2,MEA}$	-2997.52
a_{MEA,H_2O}	2.7657 [a]	b_{MEA,H_2O}	-1147.8744 [a]
a_{MEA,CO_2}	1.62828	b_{MEA,CO_2}	-1616.26

Molecule-Salt Parameters: $a_{m,c/a}$ and $b_{m,c/a}$			
$a_{H_2O,MEAH^+/MEACOO^-}$	-12.4523 [a]	$b_{H_2O,MEAH^+/MEACOO^-}$	1017.78 [a]
$a_{CO_2,MEAH^+/MEACOO^-}$	-8.92601	$b_{CO_2,MEAH^+/MEACOO^-}$	-4129.05
$a_{MEA,MEAH^+/MEACOO^-}$	-13.7033	$b_{MEA,MEAH^+/MEACOO^-}$	-2761.98

Salt-Molecule Parameters: $a_{c/a,m}$ and $b_{c/a,m}$			
$a_{MEAH^+/MEACOO^-,H_2O}$	1.7486 [a]	$b_{MEAH^+/MEACOO^-,H_2O}$	-496.199 [a]
$a_{MEAH^+/MEACOO^-,CO_2}$	8.29695	$b_{MEAH^+/MEACOO^-,CO_2}$	-3157.30
$a_{MEAH^+/MEACOO^-,MEA}$	14.6325	$b_{MEAH^+/MEACOO^-,MEA}$	-3310.86

[a] Adopted from Putta et al. [13].

Table 2: e-NRTL parameters of the long range terms for the system MEA + CO$_2$ with water being apparent for the reference state of infinite dilution.

Distance of closest approach ρ_{Dist}	14.9 [b]
Born radius r_{Born}	$3 \cdot 10^{-10}$ [a]

Dielectric constant parameters [14]: $D_i = A_i + B_i(1/T - 1/C_i)$

i	A_i	B_i / K	C_i / K
H$_2$O	78.54	31989.38	298.15
CO$_2$	1.6	0	298.15
MEA	35.76	14836	273.15

[a] Adopted from Putta et al. [13].
[b] Adopted from Pitzer [20].

Table 3: Experimental density data for the MEA + CO_2 system at various temperatures.

α / (mol CO_2 / mol MEA)	ρ / (kg/m^3)				
	313.15 K	323.15 K	333.15 K	343.15 K	353.15 K
0.12	1075	1068	1061	1054	1046
0.22	1137	1130	1124	1117	1110

Table 4: Measured Henry's constant for CO_2 in water.

T / K	H_{CO_2} / (kPa m^3 mol^{-1})
303.14	3.40
303.14	3.44
313.16	4.26
313.16	4.33
323.16	5.16
323.17	5.26
333.17	6.07
333.18	6.21
343.19	7.02
343.19	7.15
353.27	7.89
353.14	7.94
363.18	8.56
363.13	8.75
373.16	9.31
373.20	9.59
393.22	10.45
303.14	3.40
303.14	3.44
313.16	4.26

Table 5: Experimental vapor-liquid equilibrium data for the MEA + CO₂ system. In the table, T is temperature, p is pressure, α is the CO₂ loading with the combined standard uncertainty $u_c(\alpha)$ and w_{CO_2} is the mass fraction of CO₂ in the loaded solution with the combined standard uncertainty $u_c(w_{CO_2})$.[a]

T / K	p_{tot} / kPa	p_{CO_2} / kPa	α / (mol CO₂ / mol MEA)	$u_c(\alpha)$ / (mol CO₂ / mol MEA)	w_{CO_2}	$u_c(w_{CO_2})$
333.15	2.5					
333.15	3.8	1.4	0.391	0.01	0.2199	0.0002
333.15	4.6	2.1	0.422	0.01	0.2333	0.0002
333.15	8.4	5.9	0.458	0.01	0.2480	0.0002
333.15	19.9	17.4	0.480	0.01	0.2568	0.0002
333.15	80.3	77.9	0.503	0.01	0.2659	0.0002
333.15	351.5	349.0	0.528	0.01	0.2754	0.0002
353.15	3.8					
353.15	6.4	2.6	0.375	0.02	0.2127	0.0003
353.15	13.0	9.2	0.423	0.02	0.2336	0.0003
353.15	52.8	49.0	0.468	0.02	0.2523	0.0003
353.15	124.2	120.4	0.487	0.02	0.2598	0.0003
353.15	201.6	197.8	0.497	0.02	0.2636	0.0003
353.15	305.5	301.6	0.505	0.02	0.2668	0.0003
353.15	397.2	393.3	0.510	0.02	0.2688	0.0003
353.15	462.1	458.2	0.513	0.02	0.2699	0.0003
353.15	492.9	489.1	0.515	0.02	0.2704	0.0003
373.15	9.3					
373.15	10.8	1.4	0.238	0.01	0.1465	0.0002
373.15	19.5	10.2	0.353	0.01	0.2029	0.0002
373.15	33.5	24.2	0.395	0.01	0.2215	0.0002
373.15	44.3	35.0	0.410	0.01	0.2282	0.0002
373.15	76.5	67.2	0.435	0.01	0.2385	0.0002
373.15	116.6	107.3	0.450	0.01	0.2448	0.0002
373.15	225.5	216.2	0.470	0.01	0.2531	0.0002
373.15	306.8	297.5	0.479	0.01	0.2564	0.0002
373.15	361.0	351.7	0.483	0.01	0.2581	0.0002
373.15	398.0	388.7	0.485	0.01	0.2591	0.0002
373.15	9.2					
373.15	17.4	8.2	0.323	0.01	0.1887	0.0002
373.15	37.5	28.3	0.398	0.01	0.2229	0.0002
373.15	81.0	71.9	0.436	0.01	0.2391	0.0002
373.15	253.8	244.6	0.474	0.01	0.2545	0.0002

[a] Standard uncertainties u are $u(T) = 0.1$ K and $u(p_{tot}) = 0.9$ kPa, and the combined standard uncertainties u_c is $u_c(p_{CO_2}) = 1.3$ kPa. Due to small variations in α, three decimals are given.